Developmental Biology 340 (2010) 134–144

Contents lists available at ScienceDirect

Developmental Biology

journal homepage: www.elsevier.com/developmentalbiology

Evolution of Developmental Control Mechanisms

Key steps in the morphogenesis of a cranial placode in an invertebrate chordate, the tunicate *Ciona savignyi*

Matthew J. Kourakis, Erin Newman-Smith, William C. Smith *

University of California, Santa Barbara, Department of Molecular, Cell and Developmental Biology, USA

ARTICLE INFO

Article history:
Received for publication 17 October 2009
Revised 13 January 2010
Accepted 14 January 2010
Available online 22 January 2010

Keywords:
Atrial siphon primordium
Placode morphogenesis
Otic placode
Chordate evolution

ABSTRACT

Tunicates and vertebrates share a common ancestor that possessed cranial neurogenic placodes, thickenings in embryonic head epidermis giving rise to sensory structures. Though orthology assignments between vertebrate and tunicate placodes are not entirely resolved, vertebrate otic placodes and tunicate atrial siphon primordia are thought to be homologous based on morphology and position, gene expression, and a common signaling requirement during induction. Here, we probe key points in the morphogenesis of the tunicate atrial siphon. We show that the siphon primordium arises within a non-dividing field of lateral–dorsal epidermis. The initial steps of atrial primordium invagination are similar to otic placode invagination, but a placode-derived vesicle is never observed as for the otic vesicle of vertebrates. Rather, confocal imaging reveals an atrial opening through juvenile stages and beyond. We inject a photoactivatable lineage tracer to show that the early atrial siphon of the metamorphic juvenile, including its aperture and lining, derives from cells of the atrial placode itself. Finally, we perturb the routing of the gut to the left atrium by laser ablation and pharmacology to show that this adaptation to a sessile lifestyle depends on left–right patterning mechanisms present in the free-swimming chordate ancestor.

Introduction

Until recently, the vertebrate crown group within chordates was thought to be characterized by at least two unique features, ectodermal neurogenic placodes and migrating neural crest cells. Together, these contribute to the complexity of the vertebrate cephalic sensory apparatus, so much so that neural crest and placodes were said to help to form a "new head" (Butler, 2000; Northcutt and Gans, 1983; Shimeld and Holland, 2000). Cephalochordates which, until recently, had long been thought to be the sister group to the vertebrates, lack placodal structures and have a head of arguably lower complexity than vertebrates. Tunicates, or urochordates, which had been assigned the basal node of the extant chordates, were largely overlooked with respect to these features as they were believed not to share as recent an ancestry as cephalochordates and vertebrates (but see (Jefferies, 1986; Wada et al., 1998). They also display a host of derived features, including a seemingly simplified embryogenesis with fewer cells that follow a more determinative development, a radical metamorphosis resulting in a sessile, filter feeding adult, and the ability to make cellulose — a macromolecule often associated with plants. Our view of chordate phylogeny has been revised over the past several years, however, and widely accepted phylogenies now place tunicates as the nearest ancestor to the vertebrates, with the cephalochordates as the outgroup (Blair and Hedges, 2005; Delsuc et al., 2006; Putnam et al., 2008).

In spite of their many unique features, the marine-dwelling tunicates show many general chordate attributes – notochord, dorsal nervous system, and muscular tail – during a brief swimming larval phase, and others, such as a pharyngeal basket perforated with gill slits, after metamorphosis. While tunicates and vertebrates have both undergone modification since their common ancestor, there are important anatomical traits that ally them, traits thought to have appeared after the divergence of the cephalochordates from the vertebrate–tunicate lineage. Among these are neural crest or crest-like cells (Jeffery, 2006; Jeffery et al., 2008), and the topic of this paper, neurogenic placodes — focal thickenings within epidermis in the head region that give rise to sensory structures. Vertebrate placodes include otic, olfactory, hypophyseal, lens, trigeminal, epibranchial, lateral line, and profundal placodes (Schlosser, 2005). In vertebrates, some examples of placodal derivatives are components of the inner ear, olfactory epithelium, head ganglia, and the lateral line of fish and some amphibians. Putative tunicate placodes are thought to include the stomodeal placode, the rostral placode giving rise to the adhesive palps, the adenohypophyseal placode, and the paired atrial siphon primordia. Tunicate placodal structures have been the subject of more recent investigations with some emphasis given to their possible homology to vertebrate placodes (Manni et al., 2004; Mazet et al., 2005). Strict relationships can be difficult to assign because there are more vertebrate placodes than tunicate placodes, and hence, no clear one-to-one correspondence. Moreover, there may have been significant

* Corresponding author.
E-mail address: w_smith@lifesci.ucsb.edu (W.C. Smith).

0012-1606/$ – see front matter © 2010 Elsevier Inc. All rights reserved.
doi:10.1016/j.ydbio.2010.01.016

heterotopic changes between tunicate and vertebrate lineages. For example, Manni et al. have contended that the coronal organ, derived from the stomodeal (mouth) placode and bearing secondary mechanoreceptor hair cells, may offer evidence that the mouth of ascidians, a class of tunicates, contains elements homologous to derivatives of the vertebrate acoustico-lateralis system, i.e., derivatives of otic and lateral line placodes of vertebrates (Manni et al., 2006).

Among the strongest cases for homology between vertebrate and tunicate placodes is the relationship between the vertebrate otic placode and the ascidian atrial primordium. Both appear during early development as bilaterally paired structures anterior to the notochord at about the level of the hindbrain (in some ascidians a single unpaired dorsal placode is present; this likely represents a derived condition, see below). Both express a similar battery of gene markers including, e.g., *Dll-A*, *Six1/2*, *Eya*, *Pax 2/5/8*, and *Fox* genes, defining a signature pattern for otic and atrial placodes (though no single gene has been described that is expressed in the otic or atrial primordia and nowhere else) and both require Fgf during induction (Caracciolo et al., 2000; Irvine et al., 2007; Kourakis and Smith, 2007; Mazet et al., 2005). Moreover, both the vertebrate otic placode and the ascidian atrial primordium undergo invagination leading to the elaboration of specialized adult head structures including a connection between epidermal derivatives with the endodermal tissue of the pharynx. Both also appear to be neurogenic. Otic placode derivatives include the stato-acoustic ganglion, maculae of the utricle and saccule, and the hearing receptors of the cochlea, the Organ of Corti. Ascidians have been found to have sensory hair cells somewhat resembling lateral line neuromasts within the adult atrium (Bone and Ryan, 1978). However, neurogenic markers are absent before metamorphic stages in *Ciona* and these hair cells have not been traced as descendents of the atrial epithelium (Mazet and Shimeld, 2005); additionally, these cells are not secondarily innervated as in vertebrates, but have their own axons (Bone and Ryan, 1978).

In vertebrates, the otic placode gives rise to structures of the vertebrate ear and forms a connection to the pharynx via the otopharyngeal tube. In ascidians, the atrial primordium is the larval precursor to the adult atrial siphon (Figs. 1A and B), the excurrent route through which both waste and gametes are directed in post-metamorphic life, and likewise forms in close relation to the pharynx. While previous investigations have bolstered otic/atrial homology by demonstrating similar gene expression patterns for an extensive battery of ascidian orthologs to vertebrate otic placode expressed genes, and probing the functional requirements of atrial primordium development, the morphology of the atrial primordium itself or its descendents during development have been less well studied (but for an extensive treatment of gill slit formation in post-metamorphic animals and an overview of placode types, see (Manni et al., 2004, 2002).

The later events in vertebrate ear formation including the elaboration of the inner ear are not easily likened to atrial development in ascidians, but the induction of the placode, its subsequent invagination, and its integration with underlying pharyngeal endoderm are likely similar due to shared ancestry of vertebrates and ascidians. One report indicates that cyst or vesicle formation, by means of a pinching off of the invaginated ectoderm from the surface, is yet another element in common between vertebrates and ascidians (Manni et al., 2004). This feature was reported during the larval phase of *Ciona*, with a new opening reconnecting the vesicle to the exterior after gill slit formation, near the end of metamorphosis. The tissue contributions to the tunicate atrial complex (the collection of structures that make the mature atrial siphon, including the atrial aperture, the walls of the atrial cavity, and the gill slits) is less clear than for vertebrates in spite of this structure's relative simplicity. While the primary tissues involved are thought to be the surface ectoderm of the placode and the underlying pharyngeal endoderm that may receive instructive cues from the ectoderm during gill slit formation, the precise contributions by the atrial placode itself have not been determined; previous data that may be informative for this question are derived from different ascidian species and appear contradictory, these results will be discussed below.

We address aspects of both early and later atrial primordium morphogenesis in the ascidian *Ciona savignyi* including atrial primordium/placode formation and invagination leading to the formation of the atrial cavity. We focus, in particular, on the timing of the initial appearance of a distinct morphological primordium within a field of lateral epidermal cells during embryonic tailbud stages and show that this structure is visible hours earlier than previous reports. We examine the first signs of invagination of this structure and observe that the process of invagination does not include vesicle or cyst formation, as in vertebrates, but instead is characterized by a persistent connection to the exterior. We map the fate of cells of the atrial primordium using a photoactivatable caged fluorophore and show that cells of the placodal ectoderm fate to all portions of the atrial siphon, up until the anatomical boundary separating peribranchial

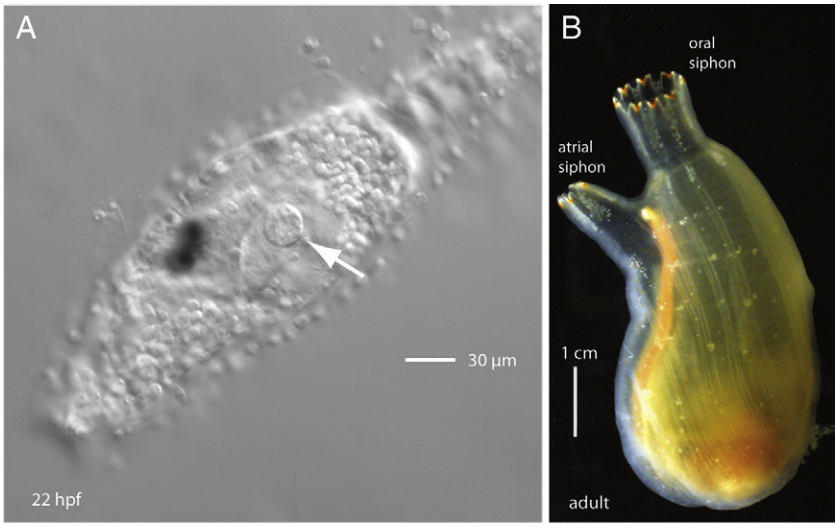

Fig. 1. The atrial primordium in *Ciona* development. (A) Lateral view of the head and trunk region of a *Ciona savignyi* larva, about 3 h after hatching (anterior is left). The left atrial primordium is visible as a disk on the lateral epidermis (arrow). (B) An adult ascidian showing the single atrial siphon branching slightly to the left and the larger oral siphon, top center. The oral siphon arises from a single rudiment, whereas the adult atrial siphon results from the fusion of paired juvenile atrial siphons.

(atrial side) from branchial (pharynx side) epithelia. We use the fate mapping data to attempt to reconcile seemingly conflicting data from previous investigators, and in this attempt, propose a model for the interaction of the invaginating atrium with the endodermal epithelium of the pharynx. Additionally, we show that an accessory function of the post-metamorphic left atrial siphon, the exit point for the intestine, depends on a common chordate left–right patterning mechanism during embryogenesis.

Materials and methods

C. savignyi

C. savignyi were collected at the Santa Barbara yacht harbor and transferred to a holding facility at the University of California, Santa Barbara that is supplied with raw seawater. Individual animals were transferred to a constant light room for 2–5 days so that their gametes would accumulate. Animals were crossed by combining gametes for about 15 min after dissection. Fertilized eggs were washed with seawater and kept at 18 °C.

When necessary, animals were dechorionated using as previously described (Kourakis and Smith, 2007). Gametes from separate individuals were combined, allowed to sit for 15 min at 18 °C, then washed into dechorionation solution in a petri dish where they were gently agitated with aspiration by pasteur pipette until separated from their chorions, about 5 min. Dechorionated eggs were then washed in seawater in agarose-coated dishes, changing dishes three times and allowed to develop until they reached the desired stage.

Live embryos were imaged with differential interference contrast (DIC) optics. Embryos for timelapse photography were dechorionated and bisected to remove the tail so that they would remain immobile. Specimens were imaged by confocal microscopy using an Olympus Fluoview 500. Animals were fixed in 2% formaldehyde in seawater for 1 h then washed in PBT, stained with BODIPY phallacidin (1:200) and DAPI or DRAQ5 (1:1000), cleared in 2:1 benzyl alcohol:benzyl benzoate, then mounted.

Caged fluorescein

Caged fluorescein dextran (10 K MW) (Molecular Probes; product discontinued) was injected at the 1-cell stage. Animals were kept in the dark at 18 °C until just after hatching (about 20 h). To uncage the fluorophore, larvae were placed in 0.04% tricaine, diluted 1:10 in seawater, and mounted on slides under cover slips. A foil pinhole was placed over the field diaphragm to allow the area of fluorescent illumination to be restricted to an approximately 5 μm radius when viewed through the 40× objective. Illumination under ultra violet (uv) wavelength allows the caging moiety to release the fluorophore. Samples were uncaged for about 1 s under uv, confirmation of uncaging was visualized with a fluorescein isothiocyanate filter set. Selected animals were then removed from the slides, placed back in seawater in the dark and allowed to progress through metamorphosis and visualized live.

Laser ablation

A dye-laser was used to ablate cells of the atrial primordium as described previously (Kourakis and Smith, 2007).

Pharmacology

U0126 was used as described (Kourakis and Smith, 2007). Omeprazole (Sigma) was diluted in DMSO to a stock concentration of 20 mg/mL. A working concentration was made by diluting to 40 μg/mL in seawater. *C. savignyi* were treated with omeprazole from gastrulation through to late neural stage, chorion intact, then washed in seawater and allowed to develop normally. As a control, siblings embryos were treated in the same manner with 12 μL DMSO in 3 mL seawater.

Results

Visualization of early placode coalescence and formation

Previous descriptions of the atrial primordium focus on the period shortly after hatching, when the placodal structure is easily visualized; these descriptions do not say whether the larval stage represents the primordium's first appearance, however. While the placode becomes most prominent at the larval stage, it is likely to form earlier. Only by determining the timing of formation can its appearance be meaningfully related to the timing of expression of putative placodal markers which can, in turn, inform our views on how and when specification occurs. Moreover, capturing placode formation in the live animal can reveal whether cells of the forming placode are characterized by such general properties as migration or division. To determine when the placode first formed, we used DIC optics and followed live animals through embryonic and larval development. At late neurula to early tailbud, the *Ciona* embryo develops a distinct trunk/tail division. The head/trunk region shows no morphological elaborations from the epidermis at this stage, i.e., no palps are visible. Before the appearance of the pigmented cells of the sensory vesicle, mesenchyme in the left and right trunk lateral regions becomes more prominent, forming broad lateral protuberances [For a detailed staging series of *Ciona* development, see (Hotta et al., 2007). This staging series is based on observations of *Ciona intestinalis*; we see no significant differences in the development of *C. savignyi*.] Timelapse imaging during these stages with DIC optics on either right or left lateral flanks shows a field of epidermal cells with no atrial primordium, roughly homogeneous in composition. Timelapse over a few hours reveals that these cells do not shift or move with respect to one another and that there is little or no cell division within the lateral field of cells (more anterior portions of the epidermis, from the future site of the oral primordium to the rostral tip, were not analyzed).

When the first pigmented cell, the otolith, is visible, at approximately 12 hours post fertilization (hpf) (Hotta stage 23), the lateral trunk epidermis remains roughly homogeneous and shows no placodal structure. At stage 24, about 1.5 h later, the tail of the dechorionated embryo begins to straighten relative to the trunk. Shortly after this a coalescence of several epidermal cells is seen in the dorsal lateral portion on both right and left sides. These cells gain a clear outer boundary that encloses them in a disk of epidermal cells (Figs. 2A and B and Supplementary movie). This structure is the incipient atrial primordium; which is visible about 2–3 h earlier than reported previously [see e.g., (Hotta et al., 2007; Katz, 1983; Mazet and Shimeld, 2005)]. The number of cells appears to be six, although this number was difficult to determine at the time of demarcation of the outer placode boundary. However, we never observed it to include fewer than five cells, in agreement with earlier estimates made about the number of cells in this structure (Katz, 1983). At approximately 16 hpf (stage 25), after melanization of the ocellus is observed, we counted six cells in the visible surface primordium, using DIC optics to locate nuclei (Figs. 2C and D). Additionally, by this stage, the cells had assumed a ring arrangement, the abutting inner faces of the adjacent cells forming the vertices of an internal hexagonal aperture, supporting the notion that six cells characterize the surface of newly formed atrial placode.

Invagination of atrial primordium and persistence of the atrial aperture

The cells of the atrial primordium, like the epithelium of the vertebrate otic primordium (and the epithelia of other, but not all, vertebrate placodes) eventually begins invagination. It might be

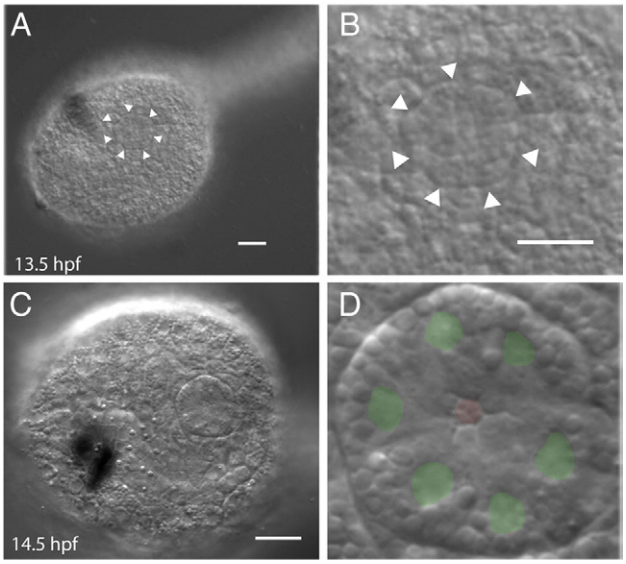

Fig. 2. (A) First appearance of the atrial primordium in *Ciona* tailbud embryos. At about 13 h post fertilization the *Ciona* tail begins to straighten. About 30 min later, a distinct circular cluster of cells with a clearly defined border appears in the epidermis. (B) Detail of lateral trunk epidermis in A. (C) DIC image showing surface epidermis of recently formed atrial primordium. (D) Detail of C with green where nuclei are observed and a red hexagon at the central aperture of the atrial primordium. Scale bar = 20 μm.

expected that the atrial placode would not invaginate until after metamorphosis, at which time a functional connection with the pharynx through the gill slits is established, and filter feeding begins. Our observations show, however, that the placode invaginates soon after its formation. In the later tailbud embryo (about stage 25), viewed from the dorsal aspect, right and left placodal structures can be seen to invaginate slightly, forming a shallow cup (Fig. 3A). This represents invagination in the strict sense, a folding inward of the surface cells. We note that in *Ciona*, the timing of invagination is approximately coincident with the first phase of vacuolization of the notochord, when well-formed luminal pockets are evident throughout the notochord, but before a continuous lumen has formed (Dong et al., 2009) — in timelapse, the anterior portion of the notochord was seen to extend slightly forward during this period.

By the time the embryo has hatched, the primordium is visible as a discrete bolus of cells just below the level of the surface ectoderm. Confocal sectioning to allow counting of individual nuclei shows twelve nuclei in the primordium, consistent with one round of cell division since its formation. Even at this later stage, the opening that defines the proximal portion of the incipient atrium persists, so that the atrium remains topologically continuous with the outer trunk epidermis. At this stage, the cell bolus shows a clearly defined boundary at its outer edge, with cell nuclei occupying the portion of the cell closer to the atrial cavity; cells closest to opening are narrower and compressed, forming a hinge with the non-placodal cells of the exterior (Fig. 3B). A few hours later, in swimming larvae whose synchronous siblings are readily able to attach to the substrate and undergo metamorphosis, we continue to observe a relatively narrow, shallow, but well-defined atrium which remains open to the outside (Fig. 3C). In mature larvae, the actin-specific phallacidin signal reveals a tight ring around that portion of the atrial passage that lies just beneath the atrial opening (Fig. 3D). If we place larvae in an agarose-coated dish so that they cannot attach and observe them at 48 h post-hatching, we note that even this late in the larval phase, the atrial opening persists (data not shown). This is significant because these animals are characterized by the precocious development of at least some features that are normally prominent only after the first phase of metamorphosis, e.g., endostyle, open stomach cavity and intestinal lumen, increased volume in the pharynx, and invaginating stomodeum. While these animals are termed "delayed" in the laboratory, presumably attachment in the wild occurs over a broad range of times post-hatching, both early and later, depending on the availability of substrate.

After metamorphosis begins but before reorientation of the visceral organs and expansion of the pharynx, the atrial aperture persists (Fig. 4A). Visceral rotation follows but the atrial aperture, though narrow and constricted in fixed samples, is maintained (Fig. 4B). The tight actin bundles around the circumference of the atrial aperture, first observed during larval stages, resolve to wider concentric rings during metamorphosis (Fig. 4C). The atrial aperture is maintained through to the 2nd ascidian stage (Berrill, 1947; Chiba et al., 2004) and beyond, when right and left chambers fuse, forming a single atrium following regression of a shared septum along the dorsal midline (Figs. 4D and E).

Fate mapping of atrial primordium precursor cells

The fate of the atrial primordium has not been directly determined. Work in two other ascidians, *Halocynthia roretzi* and *Botryllus schlosseri*, yields different conclusions about the possible placodal contribution to the atrium (Hirano and Nishida, 2000; Manni et al., 2002). Briefly, endodermal lineage tracing in *H. roretzi* shows the peribranchial epithelium as endodermally derived whereas electron micrographs of *B. schlosseri* show it as a derivative of invaginated epidermis. These results have implications for the morphogenetic movements of epithelia needed to reach a final configuration of endoderm and ectoderm around the branchial (pharynx side) and peribranchial (atrial side) epithelia. The data from *H. roretzi* were interpreted to show that ectoderm and endoderm meet near the opening of the siphon and that the gill slits form within an endodermal epithelium while the data from *B. schlosseri* imply simple apposition of the two tissues at the point where branchial fissure or gill slit formation occurs. These two species are believed to be more

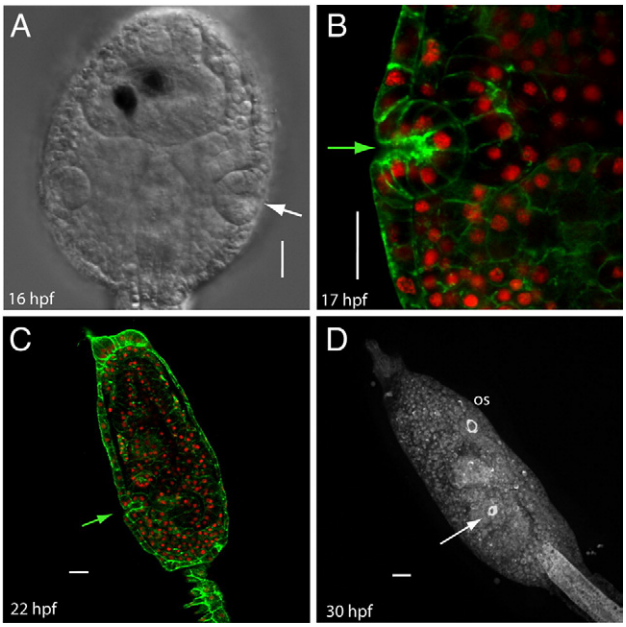

Fig. 3. Atrial invagination occurs soon after primordium formation. (A) At about 16 hpf, a dorsal view shows an invaginated primordium with incipient atrium. Anterior is up. Pigmented cells within the sensory vesicle are visible, central midline canal is dorsal nervous system; notochord is not visible in this view. (B) An optical section through a larval primordium reveals a shallow atrium (F-actin is green and nuclei are red). (C) Confocal section of a *Ciona* larva after head elongation. Arrow shows atrial aperture. (D) Fluorescent label reveals that the mature larva has a ring of actin at the atriopore. Arrow points to the atrial aperture; a similar arrangement of actin is found at the oral siphon opening (os). Scale bar = 20 μm.

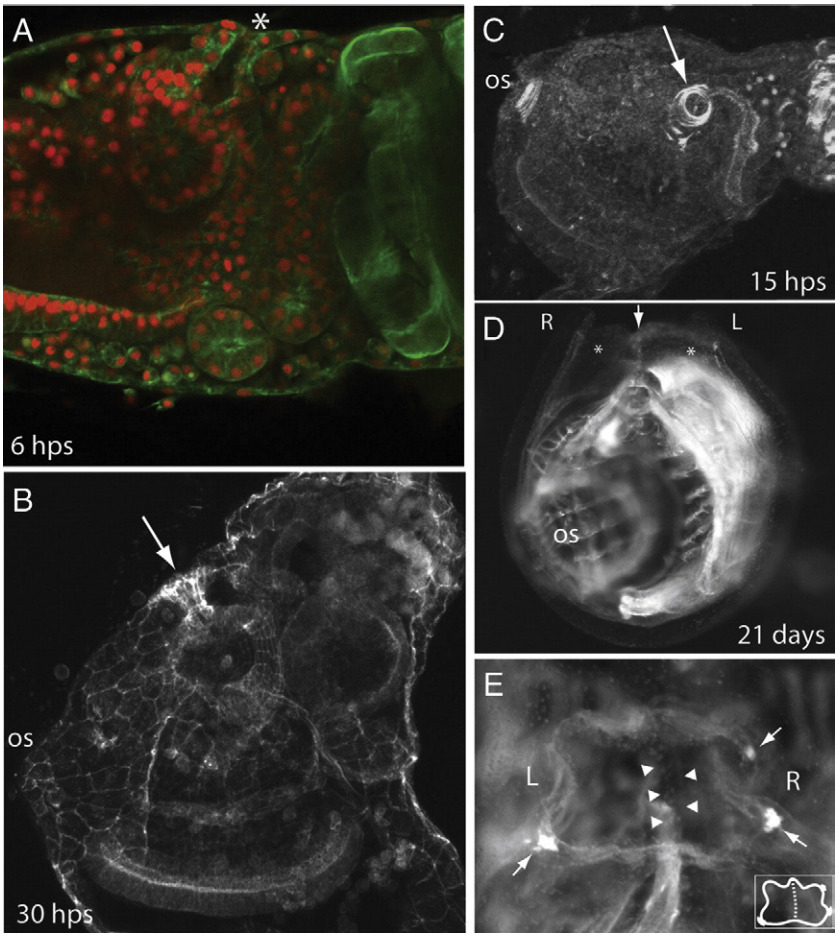

Fig. 4. The atrial aperture persists through larval and post-metamorphic development in *Ciona*. (A) Early juvenile, 6 hours post settling (hps), open atrium is at top indicated by asterisk. Actin is green, nuclei are red. (B) Average intensity projection showing actin staining in a later juvenile following gill slit formation. Arrow indicates a constricted, but open channel connecting the now enlarged atrium to the exterior. (C) After metamorphosis, the circum-atrial actin that was organized in a tight ring during later larval life resolves to concentric rings. (D) Fusion of right and left atria defines the 2nd ascidian stage. Dark-field microscopy shows a front view of a 21 day post settlement (dps) juvenile; oral siphon above the plane of the image. Left and right atria are indicated by asterisks and a common septum is indicated by an arrow. (E) Dorsal (top) view of a juvenile 21 days after settling. Left and right atrial siphons have fused to form a common siphon with only a shared, but regressing septum as a remnant their separation (arrowheads). Bright spots around edge mark the first formed pigment spots (arrows) of the fused atrium. Inset shows a cartoon schematic of the same view with the shared septum depicted as a dashed line.

closely related to one another than either is to *Ciona* (Turon and Lopez-Legentil, 2004). The colonial *Botryllus*, however, broods its larvae, and may show differences in developmental timing compared to species with free-swimming larvae (Burighel and Cloney, 1997).

We used cell labeling to directly determine the lineal contribution of the atrial primordium to the atrial complex in *Ciona*. Because the atrial primordium arises late in embryogenesis when cells are small – the atrial placode itself is only about 27 µm in diameter (Fig. 5A), consisting of a disk of 5 or 6 wedge shaped cells – standard methods for injecting tracers were not feasible. Instead, we relied on a photoactivatable dye to trace the descendent fates of only those cells we wished to follow. Caged fluorescein was injected as a lineage tracer in the single-cell embryo of *Ciona* so that after subsequent divisions all cells of the embryo would contain the caged fluorophore. The fluorescein was uncaged unilaterally in a single right or left atrial primordium (consisting of approximately twelve cells at the time of uncaging) allowing fluorescence to be observed in descendent cells (Figs. 5B–D), with the contralateral side serving as a control. Larvae went through metamorphosis and were observed at about 48 h post-hatching. The post-metamorphic juvenile at this stage shows a predictable and stereotypical anatomy (Figs. 6A and B). Fluorescence was seen in the atrium on the side where uncaging had been performed in the larval primordium. From the exterior, the ring forming the atrial aperture was positive for fluorescence (Figs. 6C and D). Detail views also show fluorescence in the inner surface of the atrium proper, extending to the gill slits at the base of the atrium, including the small space between the gill slits, the tongue bar (Figs. 6E–H). In Figs. 6I and J, we summarize the contribution of the atrial primordium descendents to the juvenile atrial complex, based on the uncaging results.

The tail rudiment always showed marked autofluorescence, evidenced in uninjected animals. In injected animals, the uncaging process was brief (less than 1 s) but the uv point source is expected to scatter somewhat. When the larval atrial primordium is exposed to pinpoint uv, the primordium is positioned over the posterior-most area of trunk endoderm, including anlagen for stomach, esophagus, and intestine (Katz, 1983). Correspondingly, experimental animals occasionally showed fluorescence in a portion of the juvenile intestine and esophagus. However, the area of endoderm fated to underlie the juvenile atrium, namely that portion of pharyngeal endoderm involved in gill slit formation, does not underlie the atrial primordium at the larval stage when uncaging was performed (Katz, 1983). We never observed fluorescence above background levels in the branchial epithelium of the pharynx, and so we believe it unlikely that signal *within* the atrium was derived from the endodermal lineage. In other words, the extent of fluorescent labeling closely matched the anatomical extent of the atrium itself, that is the entirety of the atrial cavity including the peribranchial portion of the gill slits. These results show that the fate of the atrial placode in *C. savignyi* includes all parts of the formed

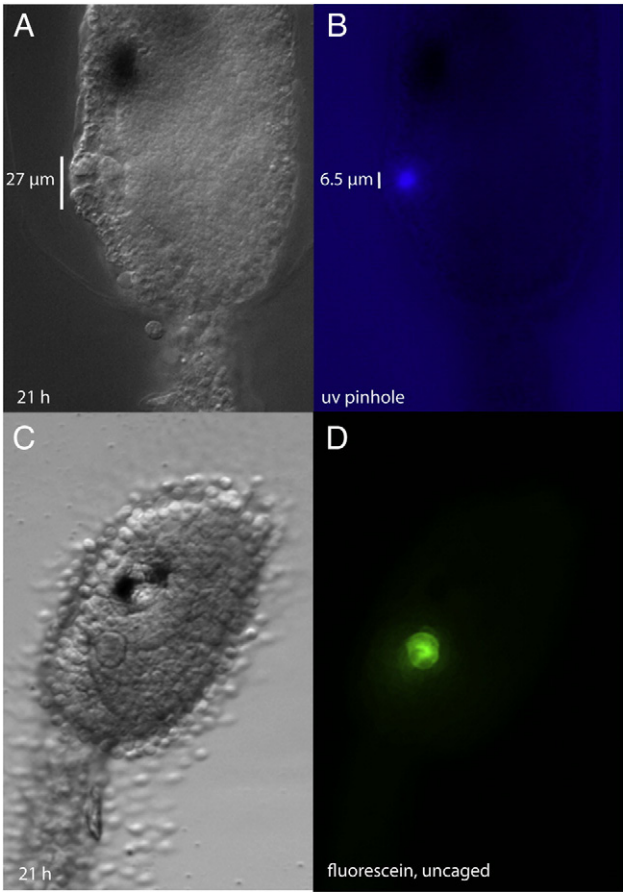

Fig. 5. UV illumination of caged-fluorescence at the early larval stage was used to label cells of the atrial primordium. (A) Live *Ciona* larva, about 21 hpf, with well-formed atrial primordium. (B) Same animal, showing the size of the uv exposure through a constructed pinhole. (C) Live *Ciona* larva after injection of caged-fluorescein and uncaging; atrium is clearly visible. The same animal viewed through the FITC channel (D), shows that the extent of uncaging closely matches the anatomical boundaries of the primordium.

atrium, from its aperture at the exterior to the gill slits at its innermost reach.

The left atrial siphon as the exit for the intestine

In most chordates, the anus is essentially a midline structure that forms at or near the site of blastopore closure in the trunk region, just anterior to the tail. In *Ciona*, blastopore closure during embryogenesis is followed by tail resorption at metamorphosis, leaving the animal without the canonical blastoporal anus for the removal of waste products. Instead, the intestine of a *Ciona* juvenile is found on the left side behind the pharyngeal basket; it turns upward and away from the holdfast and has its exit point within the left atrial cavity (Chiba et al., 2004) (Figs. 7A and B). We did not determine precisely when this asymmetry arises, but it is evident in mature or attachment-delayed larvae when feeding has not yet begun and there is no functional excretory system (Fig. 7C). In a feeding juvenile, waste from digestion is moved through the intestine, dumped into the left atrial cavity, then released through the left siphon to the exterior. We observed 200 post-metamorphic juveniles and found that the left atrium always served as the route through which the intestine exited.

This invariance towards the left atrial siphon suggested that the left atrial primordium or the siphon itself might provide attractive cues for the intestinal tract. To test this we laser ablated the larval atrial primordium shortly after hatching. These animals fail to develop left atrial siphons as juveniles, right siphons are unaffected. In a left atrial primordium ablated juvenile, we observed that the intestine remained on the left side of the animal and that the intestinal tube maintained the same pathway, with its terminus in the region near the location where the siphon and gill slits form in untreated animals (Fig. 7E). Laser ablation of the left primordium was never observed to result in a right-directed or errant intestinal tract. This indicated that the cue for the routing of the intestinal tract to the left side of the animals was not the left siphon itself.

The ablation procedure was performed after hatching, so it is possible that the left siphon primordium had already provided a left-attractive cue for the intestinal anlage. To account for the possibility of an earlier acting attractant, we took advantage of a pharmacological inhibitor of placode formation, the MEK inhibitor U0126 (Kourakis and Smith, 2007). When embryos are soaked in 10 µM U0126 at early tailbud stages, atrial primordia do not appear and most or all aspects of the atrial complex are absent including the siphon itself and gill slits. Only the inter-gill coelom, a small space formed between the two primary gill slits, is unaffected by this treatment. We observed 41 U0126-treated juveniles whose control DMSO-treated siblings had well-formed gill slits; all had scorable intestinal tracts and all of these were found on the left side and displayed the characteristic upward bend and termination point near the area where the left atrial cavity would normally reside (Fig. 7F). Because U0126 disrupts the Fgf signaling pathway and Fgf is known to play a role in left–right asymmetry (see below) (Boettger et al., 1999; Meyers and Martin, 1999), we also scored treated animals for left–right asymmetry but found no situs defects. We attribute this to the relatively late addition of the U0126, after the critical period for establishment of left–right asymmetry (Shimeld and Levin, 2006).

The embryo of *Ciona* uses the same left–right signaling pathway as in vertebrates and cephalochordates, showing left-sided expression of genes such as *pitx* and *nodal* (Boorman and Shimeld, 2002; Morokuma et al., 2002). We tested whether the routing of the intestine to the left atrial siphon might depend on this left–right pathway. *Ciona* embryos treated with omeprazole, a proton pump inhibitor, at neurula stage, show defects in left–right gene expression (Shimeld and Levin, 2006). We confirmed that this treatment also resulted in left–right anatomical defects at larval stages, scorable as left–right reversal of the pigmented otolith and ocellus. We treated animals with 40 µg/mL omeprazole from late gastrula to early tailbud stage, then placed these animals in untreated seawater and allowed them to undergo metamorphosis. In the resulting juveniles, we found that about 40% contained complete symmetry reversal (but never randomized situs defects), based on the location of anatomical landmarks such as the esophagus, heart and stomach. In all of these reversals ($n=23$), the intestine emptied into the right atrial siphon (Figs. 7H and I). We conclude that left–right patterning during the critical embryonic period determines the placement of the intestine towards the left atrium in the wildtype animal.

Discussion

Formation of the atrial siphon primordium

We show that first sign of atrial primordium formation in *Ciona* is the setting off of adjacent cells into a small, circular disk – easily visualized by the clear boundary that forms its circumference – on the dorsolateral surface of the epidermis (Figs. 2A and B). This coalescence happens rapidly, within 10 min, and does not appear to be anticipated by a similar morphologically recognizable domain, for example, of a larger size. The incipient placode appears to be composed of cells that are not the products of recent cell division. Indeed, lateral epidermal cells near the region of placode formation divide very little or not at all. This suggests that the first phase of primordium formation occurs by recruitment of cells from the epidermal field, perhaps through

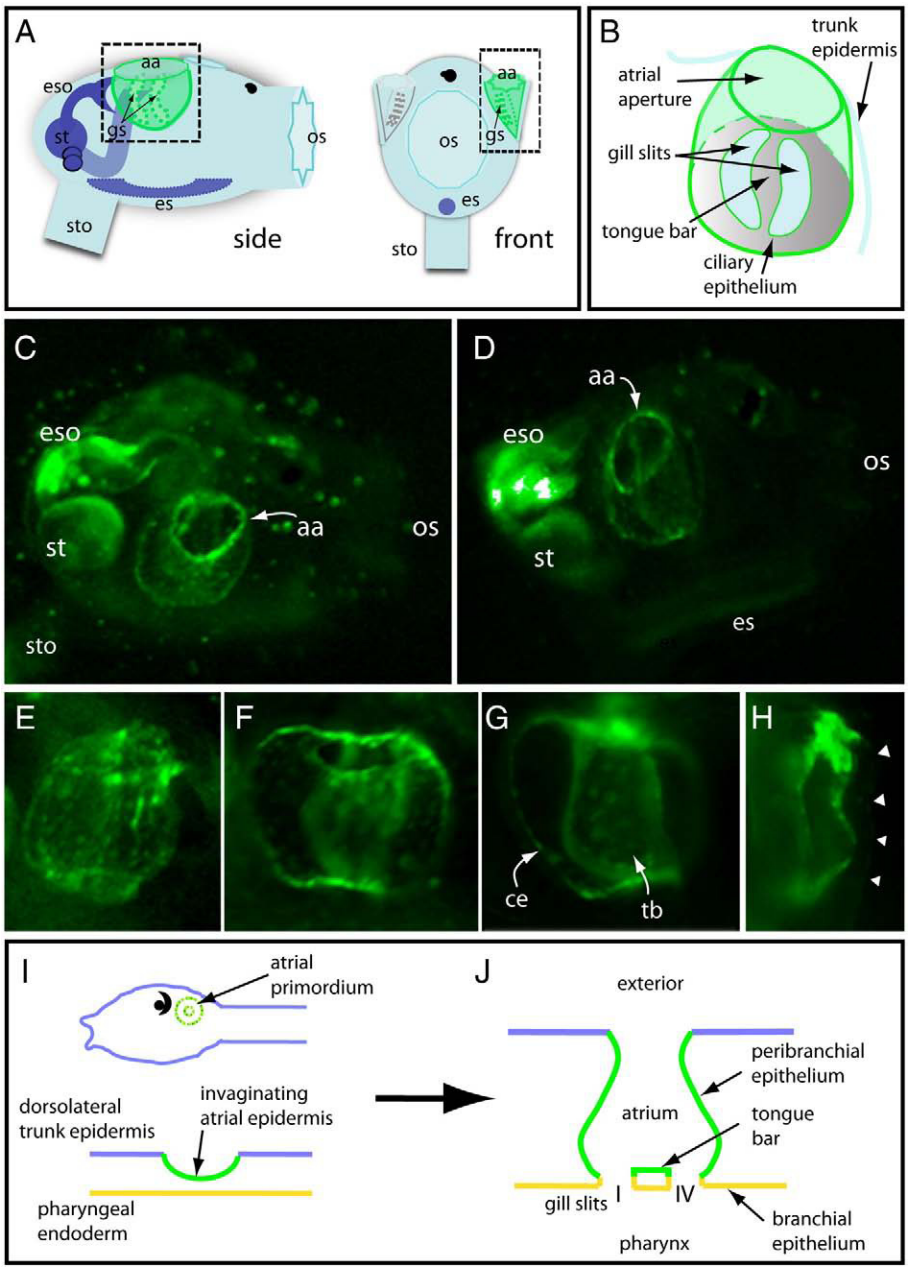

Fig. 6. Atrial primordium fates determined by caged-fluorescence. (A) Cartoon of a *Ciona* juvenile indicating its main anatomical features, including the atrial complex (shaded green). Side view is the orientation depicted for panels C and D. Dashed square on side view indicates approximate region shown in E–G. Dashed rectangle from the front view indicates view for panel H. aa, atrial aperture; gs, gill slits; eso, esophagus; st, stomach; sto, stolon; es, endostyle; os, oral siphon. (B) Cartoon detail of atrial complex showing salient features. Primary gill slits are positioned at the base of the atrium (represented as area within dotted line) and connect the atrium to the underlying pharyngeal cavity. (C) Live juvenile after uncaging in the right atrial primordium at the larval stage. The entire atrium shows fluorescence, including the bright ring marking the atrial aperture (aa). (D) Similar view of another individual after uncaging showing fluorescent label in the atrium walls, aperture, and gill slits. (E) Detailed view of a labeled atrium with punctate fluorescence in the atrium walls. Towards the top, the atrium is constricted at its aperture. (F) A labeled atrium shows that all surfaces enclosing the volume of the cavity are positive for fluorescence (G) Same animal as F, focused on the gill slits/ciliary epithelia (ce) and the tongue bar (tb) at the base of the atrial cavity. (H) Front view of an atrium shows signal in both inner and outer atrial walls with an area of intense fluorescence at the atriopore. Arrowheads indicate the outer trunk epidermis, visible through low-level background fluorescence. (I, J) Schematic showing contributions to the atrium by the placodal epidermis based on lineage tracing. Green depicts lineal contributions of the atrial primordium. Cross section of a simplified atrium (J) depicts topologies at or shortly after gill slit formation.

positional cues, and does not depend on new cell division. Our observation for the first visible signs of atrial primordium formation places this event at about 13.5 h post fertilization, earlier than previously published reports. Many investigators have included a discussion of the primordia at swimming larval stages, e.g., (Chiba et al., 2004; Katz, 1983; Mazet and Shimeld, 2005). Hotta et al. describe a morphologically visible pair of atrial primordia by stage 26, at hatching, approximately 17.5 h. In our observations, we note that after fixation the atrial primordium is more difficult to image at the time of its first appearance, perhaps due to an artifact in the surface epidermis; live specimens viewed under DIC optics always yielded more easily visible primordia.

With a revised timescale, we can reassess the correspondence between the anatomical appearance of the atrial placode and the appearance of message for *Ciona* orthologs to vertebrate placode genes, including members of the Six, Eya, Dach and Pax families. In

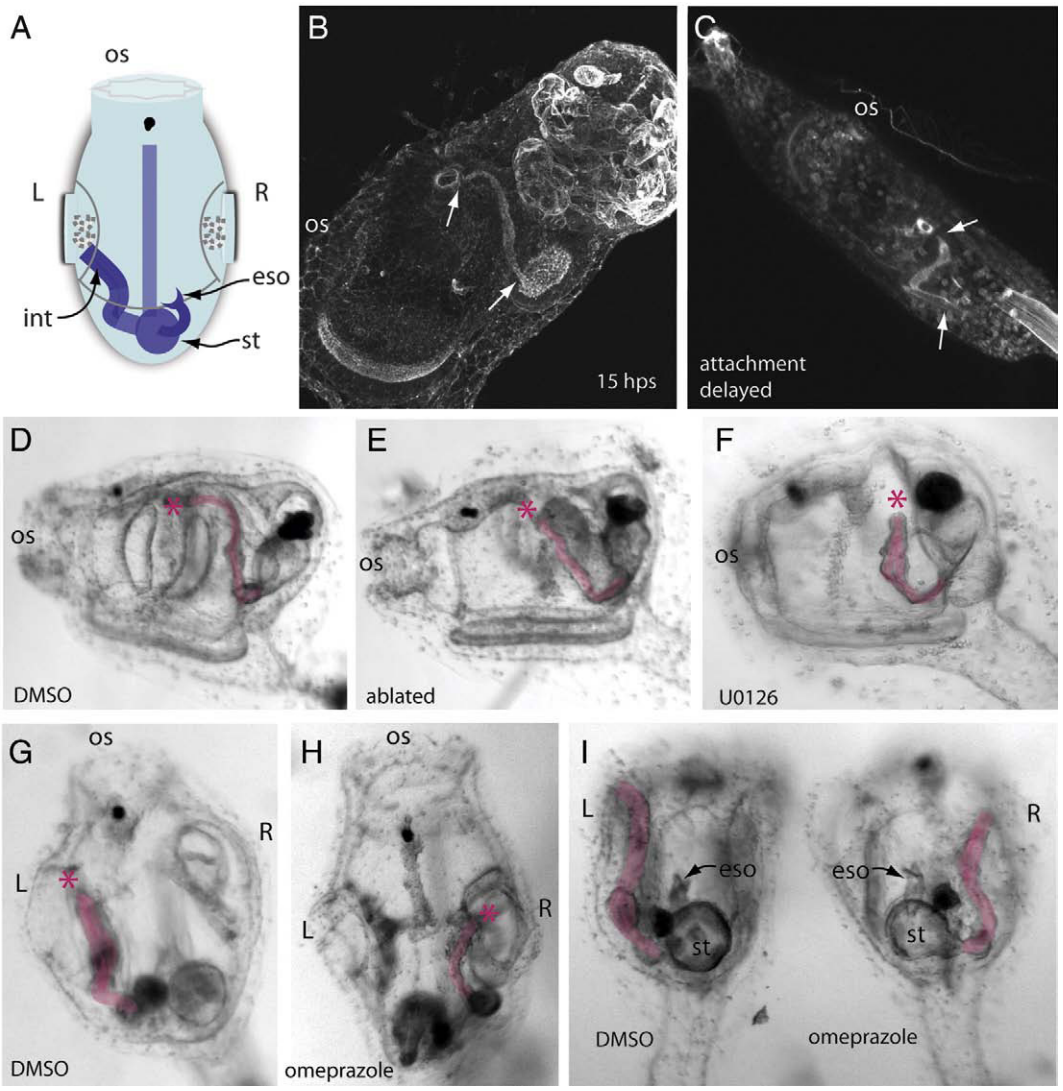

Fig. 7. The left atrium serves as the exit for the intestine in *Ciona*. (A) Schematic shows a dorsal/top view of a juvenile with some internal asymmetries depicted. os, oral siphon; int, intestine; eso, esophagus; st, stomach. (B) Confocal projection of a juvenile stained for actin. Areas of highest intensity stain are within the intestinal lumen. Arrows indicate the extent of intestine beginning just past the stomach cavity and ending near the left atrial aperture. Note the general path of the intestine upward from the aboral side towards the atrium. (C) The leftward bias of the intestine is evident even in late larval stages when the animal is not yet feeding. This confocal projection shows an attachment-delayed individual (72 h post-hatching) whose intestine terminates close to the atriopore. (D) Lateral, left view of a post-metamorphosis juvenile treated with DMSO (4 μL/mL). The intestine is highlighted. Asterisk indicates the end of the intestine. (E) When the left atrial primordium of a larva is laser ablated, no left atrium or gill slits are formed in the juvenile, but the intestine remains on the left side. (F) A 10 μM U0126 treatment in the tailbud embryo results in the loss of both right and left primordia. The resulting juvenile lacks both right and left siphons but continues to form a left-side intestine. We never observed a right-directed intestine or randomization of sidedness in these animals. (G) Dorsal view of a DMSO-treated control animal showing the leftward bias of the intestine. (H) Omeprazole treatment (40 μg/mL) results in symmetry reversal, situs inversus, with the intestine exiting the right atrium. (I) Rear view of siblings treated with DMSO or omeprazole showing that a general perturbation of right–left symmetry governs the exit path for the intestine.

vertebrate neural plate-stage embryos, many of these genes already show expression restricted to specific territories within the pre-placodal ectoderm before individual placodes are visible (Schlosser, 2002; Streit, 2007), showing that regionalization of the ectoderm precedes placode formation. In *C. intestinalis* (sister species to *C. savignyi*), orthologs to vertebrate markers are expressed at the neurula stage in mesenchyme and trunk lateral cells (Mazet and Shimeld, 2005). Later, at tailbud stages before atrial primordium formation, expression continues in underlying mesenchyme for most of these genes. This expression appears to anticipate the formation of the placodal structures in the adjacent ectoderm, although these markers demarcate a region larger than the atrial placode itself; it is plausible that the combinatorial expression of these genes may help to define a region of competence for primordium formation in the overlying epidermis. However, only later in mid-tailbud stage *Ciona* are bilateral domains of expression detected in the actual ectoderm adjacent to the visceral ganglion (Irvine et al., 2007; Mazet and Shimeld, 2005), the putative hindbrain ortholog (Canestro et al., 2005; Locascio et al., 1999; Meinertzhagen and Okamura, 2001), where the atrial primordia will form.

Our observation of an earlier timing for placode formation than reported previously suggests that ectodermal expression of putative placodal genes may only shortly precede or coincide with the formation of the placode proper. A much earlier transcription and regionalization of the epidermis, as for the multiple neighboring placodes of vertebrates (Streit, 2004), does not appear to characterize the pre-placodal region of ascidians. This timing difference might reflect that the atrial placode of *Ciona* arises singly and independently in the lateral epidermis, not in a more crowded field of placodal precursors as along the anterior neural ridge of vertebrates.

The atrial aperture

After its formation, the *Ciona* atrial aperture persists and was never observed to pinch off or seal over during any time through gill slit stage juveniles (the beginning of 1st ascidian stage (Berrill, 1947; Chiba et al., 2004)) when viewed by confocal microscopy. Atrium formation begins in the tailbud embryo soon after formation of the placode itself as a slight deflection of the inner portion of the placode toward the animal's midline when viewed dorsally (Fig. 3A). Soon after, at late embryonic and early larval stages, the atrium is observed as a small, but well-defined channel with an aperture of similar width as the cavity itself (Figs. 3B and C). Early and then later during metamorphosis (Figs. 4A and B), specimens fixed for confocal imaging showed that the opening to the atrium was constricted around its circumference, but a clear exit passage remained. We also viewed animals after gill slit formation and did not observe closure of the atrial aperture during the period until atrial siphon fusion (2nd ascidian stage). Our report differs from a previously published report of atrial development which described the developing atrium of *Ciona* as losing its aperture and becoming a closed vesicle during later larval stages; the chamber formed after vesicularization was described as reopening at the end of metamorphosis (Manni et al., 2004). Moreover, this previous report showed a closed and more extensive atrium at early juvenile stages, a feature we did not observe. We were never able to observe a vesicle or atrio-cyst and confocal imaging through several *z*-planes revealed that though the atrial aperture could be constricted toward the exterior, especially after metamorphosis and visceral rotation, a bona fide passage was maintained. Whereas our observations derive from *C. savignyi*, the report cited used the closely related *C. intestinalis*; we admit the possibility for differences in atrium morphogenesis between these species but we believe this possibility to be unlikely.

The presence of actin rings just beneath the atrial aperture was observed from larval through metamorphic stages (Figs. 3D and 4C). At the larval stage, this structure might be interpreted as a mechanism for the closing-up of the atrium at the exterior, i.e., for the vesicularization of the incipient atrium, but its continuity through to juvenile stages (along with the direct observation of a continuous passage and aperture) belies this. Moreover, in the juvenile these bundles appear to correspond to muscle fibers which are likely control aperture size by expansion and contraction. To our knowledge, the vertebrate otic cup and early vesicle contain no such arrangement of circumferential actin-rich rings; otic vesicle morphogenesis has been likened to bending of the vertebrate neural plate and neural tube closure (Mansour and Schoenwolf, 2005), which include higher concentrations of actin at the apical (luminal) surface (Ostrovsky et al., 1983).

Could the lack of vesicle or cyst formation represent the basal condition for the chordate atrial/otic primordium or is this a lineage specific loss for *Ciona*? In the colonial ascidian, *B. schlosseri*, atrium formation is different than in *Ciona*. Unlike *Ciona*, which forms paired left and right atrial primordia, *B. schlosseri* forms a single dorsal atrial placode that invaginates then bifurcates to form left and right atrial chambers. At the tailbud stage, the invagination is reported to close and separate from the epidermis; only later, during metamorphosis, does the atrium open again (Manni et al., 2004). This process is more reminiscent of vertebrate cyst formation; a chamber which is the product of invagination becomes topologically isolated from the overlying epidermis from which it originated. This similarity between *B. schlosseri* and vertebrates could indicate that cyst or vesicle formation is an ancient property of the atrial/otic placode and that vesicle formation is not a unique vertebrate character. However, it should be noted that the arrangement of a single placode in the colonial ascidian *B. schlosseri* is likely to be a derived feature, a radical heterochronic and heterotopic shift that represents a fusion of paired primordia into a single dorsal primordium at the outset of atrial formation rather than at the end, as in the solitary ascidian *Ciona*. A broader survey of atrial formation within other tunicates could help to resolve whether vesicle formation is an ancient characteristic of a chordate atrial/otic placode or a unique feature of the vertebrates. In vertebrates, the formation of the otic vesicle stands as the first step in the morphogenetic movements and cellular differentiation leading to the complexity of the inner ear including the cochlea, semicircular canals and associated sensory structures; though the ascidian atrium lacks this complexity, it may nonetheless provide clues into the ancestral ground state of this chordate placode.

Atrial primordium fate and tissue topology during gill slit formation

Although the atrial primordium of ascidians is known in general terms to be the anlage for the atrial siphon, the precise contribution of the ectodermal primordium to the post-metamorphic atrial siphon has never been directly determined. It has been demonstrated that an animal without atrial primordia, either through experimental extirpation (see Kourakis and Smith, 2007) or in mutant strains (our unpublished data), fails to form atrial siphons or gill slits. This indicates only that the atrial ectoderm is *required* for both siphon and gill slit formation, but whether the primordium is simply an inducer that will constitute only a portion of the atrium proper, or whether it is, in fact, a major lineal component of the mature atrial siphon, remained unresolved. Data from previous reports have relevance to this question: in a study of *Botryllus* gill slit formation, investigators note that electron micrographs reveal tunic cells within the developing atrium in that portion closest to the overlying surface epidermis; because tunic-bearing cells are a characteristic of the external epidermis, this portion of the atrium is likely to derive from invaginated epidermis (Manni et al., 2004). Sections through the developing atrium also show the peribranchial epithelium closest the gill slits to be continuous with the remainder of the atrium (Manni et al., 2002). This suggests a simple division of peribranchial epithelium as epidermally derived and branchial epithelium on the pharynx side as endodermally derived. Data from *H. roretzi* suggest a different arrangement, however. In *Halocynthia*, endodermal fates have been determined using horseradish peroxidase (HRP) injected into early endodermal precursors of the gastrula-stage embryo (Hirano and Nishida, 2000). After metamorphosis, HRP staining was detected in organs of the digestive system and endostyle, but also within the atrial epithelium, the peribranchial portion of the atrium including the ciliated epithelium of the gill slits. In contrast to *Botryllus*, this shows a contribution by endodermally derived cells *within* the atrium itself. The complementary labeling experiment mapping the ectodermal lineage was not performed; the authors depict the entirety of the peribranchial epithelium as endodermally derived with a transition to epidermis at the siphon exit.

Our data mapping the fate of the atrial primordium with a caged fluorophore directly show that descendent cells of the primordium are found throughout the siphon, consistent with the observations from *Botryllus*. Fluorescence is seen at the aperture of the atrium, within the entirety of the atrial (peribranchial) epithelium, including those portions between neighboring gill slits, and at the site of the gill slits themselves. Minimally, this shows that descendents of the atrial primordium constitute a major lineal component of the juvenile siphon. This suggests a model in which an ectoderm/endoderm boundary follows discrete anatomical/morphological boundaries, similar to Willey's proposal for the arrangement of these tissues (Willey, 1893). Under this schema, the atrium, including the peribranchial portion of the gill slits, is ectodermal and the branchial portion of the gill slits is endodermal, derived from endoderm of the pharynx (Figs. 6I and J). This model preserves a parsimonious topology of epithelia at the time of gill slit formation; the two epithelia come to be apposed after atrial invagination and branchial fissures form at points of contact. The patterning governing the precise location of the fissures has yet to be described, but the simple apposition of epithelia followed by

fissure suffices for the final arrangement seen in the juvenile and adult ascidian.

The apparently conflicting data from *Botryllus* and *Halocynthia* may point to species specific differences. Moreover, the data are not equivalent; for example, our own data do not directly address the presence of endoderm in the juvenile atrium, and therefore, we cannot formally rule out this possibility. Nevertheless, we believe that the topological transformations required for endodermal epithelia to occupy the atrium of the juvenile ascidian make this unlikely, especially when contrasted to simple ectoderm/endoderm apposition. In *Halocynthia*, HRP labeling were assayed at approximately one month after injection, well after the completion of metamorphosis, when many rows of gill slits had formed and the basic arrangement of early metamorphosis could have been obscured by further cell movements including, for example, the independent movement of endodermal cells which were not part of the pharyngeal epithelium underlying the invaginating atrium. It would be informative to repeat the HRP labeling with observations taken much earlier, at or shortly after formation of the primary gill slits, when primary epithelial arrangements are presumably still intact, to see whether *Halocynthia* atrium/branchial fissure formation are comparable to the other ascidian species analyzed.

The atrial complex of tunicates and the ear of vertebrates bear striking similarities; an invaginated placode forms the basis of an anatomical structure that ultimately articulates epidermis with the pharynx. However, the final topological relations of tissues comprising the vertebrate ear differ significantly from those of the *Ciona* atrial complex. In vertebrates, the otic cup closes off to become a fluid-filled vesicle and then undergoes an elaborate morphogenesis resulting in the complex inner ear. The labyrinthine derivatives of the vesicle are linked to the exterior through the ossicles of the middle ear, which abut the tympanic membrane and external auditory canal, formed by invagination of epidermis at the first pharyngeal cleft. From the interior, pharyngeal endoderm reaches the middle ear as the otopharyngeal canal (Eustachian tube) and endoderm from the first pharyngeal pouch comes to line both the canal and the middle ear. Thus, the pharynx-derived otopharyngeal canal never comes in direct contact with the inner-ear derivatives of the otic vesicle. In *Ciona*, by contrast, we propose that the pharyngeal endoderm and atrial ectoderm directly abut at the site of gill slit fissure. Additionally, crest-derived tissues and mesoderm play an important part in vertebrate ear development; it remains an open question what contribution, if any, these make to the mature atrial complex of tunicates.

The left atrial siphon as terminus for the intestinal tract

One curious feature of the sessile lifestyle of *Ciona* is the rerouting of the gut to the left atrium of the juvenile. The adoption of a post-metamorphic sessile lifestyle occurred at the base of the ascidian lineage (Wada and Satoh, 1994). Sessility brought with it a host of attendant modifications, many the direct result of metamorphosis. The pharyngeal basket has come to dominate the filter feeding ascidian's anatomy, with the larger oral siphon serving as the incurrent siphon to the pharynx. The descendent siphons of the right and left atrial primordia fuse to form a single out-current siphon, which carries water, gametes and waste to the exterior. Gametes and waste share this all-purpose atrial exit by virtue of a rerouting during evolution of what were posterior midline structures, the anus and gonoduct, to the atrium itself, with the anus opening into the left atrium. Gonoduct formation is completed later, possibly after fusion of the juvenile atria within the single shared atrial cavity (Chiba et al., 2004; Okada and Yamamoto, 1999). In the *Ciona* juvenile the completion of the gut with its exit in the atrial cavity is essential as this event roughly corresponds to the onset of feeding and comes weeks before the fusion of the two siphons.

Ablation experiments, laser or chemically induced, show that the routing of the intestine to the left side with its terminus toward the top middle portion of the left atrium does not depend on the left atrial primordium or siphon itself. Instead, this placement relies on canonical left–right signaling; in total symmetry reversals induced by omeprazole, the intestine always is found on the right side and always exits through the right atrium. Our demonstration provides confirmation for a hypothesis made previously that directional looping in the ascidian gut would depend on left–right pathway genes (Chea et al., 2005). The left-directed intestine represents a peculiar case in which the metamorphic body plan required a novel solution to the problem of waste disposal, a rerouting through the atrial siphon. In this case the solution has been, at least in part, to place the structure under the control of a more generic and ancient mechanism governing asymmetry. Intermediate forms between the presumed midline-posterior anus of a bilateral, swimming ancestor and the left atrium placed intestinal exit point for *Ciona* may not be entirely obvious but, as always, an examination of diversity within the tunicate subphylum of intestinal placement during development might help to shed light on this evolutionary transition.

The dependence of the intestine on left–right patterning could represent co-option, an older gene network put to a new use, but the placement of the terminal portion of the intestine may also simply reflect that it has been subsumed into the left–right asymmetry of all visceral organs. These organs begin as larval rudiments that are crowded, along with the mesodermal heart primordium, into the posterior portion of the trunk. The bias of the intestine toward the left side of the juvenile may in part reflect steric necessities; the intestinal rudiment cannot simply take a random direction, out either right or left atria, because of constraints created by the packing in of other organ anlagen. That an intestine routed out the right atrium is only observed in animals with total reversal (situs inversus) supports this notion.

While the routing of the intestine out the left atrium can be confidently identified as a derived characteristic within the tunicate clade, other features that are unique to either vertebrate or ascidian otic and atrial placodes are difficult to characterize as derived or ancestral without data from a third taxon. As mentioned previously, cephalochordates appear to lack placodes and the atrium of *Branchiostoma* likely does not share common ancestry with the tunicate atrium, but rather appears to be a functional analog, formed by midline fusion of ventral, metapleural finfolds with subsequent expansion of the resulting enclosed volume (Lancaster and Willey, 1890). Minimally, we can say that the common ancestor of tunicates and vertebrates had an otic/atrial placode that was similarly induced, requiring the Fgf pathway, and expressed an array of genes including orthologs to *Dll*, *Pax 2/5/8*, *Six 1/2*, and *Eya*. Invagination was a feature of this placode and was tied to interactions with endoderm of the pharynx, but whether the otic/atrial precursor formed a vesicle or maintained an open cavity throughout its development, as seen in *Ciona*, are subjects for speculation. This view assumes that the larvacean Langerhans organs share homology to the otic placode, as discussed elsewhere (Bassham and Postlethwait, 2005), but that other anatomical features, e.g., an invaginating epidermal primordium and atrial cavity associated with primary gill slits, have been lost in this lineage. Although important questions remain to be answered regarding the modification of this placode over time, the shared aspects of ascidian and vertebrate atrial/otic primordia continue to argue for their common ancestry and additionally, point to ascidians as a tractable model for investigations into early placode development.

Acknowledgments

Use of the Olympus Fluoview 500 confocal microscope at U.C. Santa Barbara is supported by an NCRR shared instrumentation grant 1510RR017753-01. Thanks to Shota Chiba for helpful comments on the manuscript. This work was supported by grants from the NIH (HD38701 and GM075049) to W.C.S.

Appendix A. Supplementary data

Supplementary data associated with this article can be found, in the online version, at doi:10.1016/j.ydbio.2010.01.016.

References

Bassham, S., Postlethwait, J.H., 2005. The evolutionary history of placodes: a molecular genetic investigation of the larvacean urochordate *Oikopleura dioica*. Development 132, 4259–4272.

Berrill, N.J., 1947. The development and growth of *Ciona*. J. Mar. Biol. Assoc. 26, 616625.

Blair, J.E., Hedges, S.B., 2005. Molecular phylogeny and divergence times of deuterostome animals. Mol. Biol. Evol. 22, 2275–2284.

Boettger, T., Wittler, L., Kessel, M., 1999. FGF8 functions in the specification of the right body side of the chick. Curr. Biol. 9, 277–280.

Bone, A., Ryan, K., 1978. Cupular sense organs in *Ciona* (*Tunicata:Ascidiacea*). J. Zool. 186, 417–429.

Boorman, C.J., Shimeld, S.M., 2002. Pitx homeobox genes in *Ciona* and amphioxus show left–right asymmetry is a conserved chordate character and define the ascidian adenohypophysis. Evol. Dev. 4, 354–365.

Burighel, P., Cloney, R.A., 1997. Urochordata: Ascidiacea. In: Harrison, F.W., Ruppert, E.E. (Eds.), Microscopic Anatomy of Invertebrates, Vol. 15. Wiley-Liss, Inc., New York, pp. 221–347.

Butler, A.B., 2000. Sensory system evolution at the origin of craniates. Philos. Trans. R. Soc. Lond., B Biol. Sci. 355, 1309–1313.

Canestro, C., Bassham, S., Postlethwait, J., 2005. Development of the central nervous system in the larvacean *Oikopleura dioica* and the evolution of the chordate brain. Dev. Biol. 285, 298–315.

Caracciolo, A., Di Gregorio, A., Aniello, F., Di Lauro, R., Branno, M., 2000. Identification and developmental expression of three Distal-less homeobox containing genes in the ascidian *Ciona intestinalis*. Mech. Dev. 99, 173–176.

Chea, H.K., Wright, C.V., Swalla, B.J., 2005. Nodal signaling and the evolution of deuterostome gastrulation. Dev. Dyn. 234, 269–278.

Chiba, S., Sasaki, A., Nakayama, A., Takamura, K., Satoh, N., 2004. Development of *Ciona intestinalis* juveniles (through 2nd ascidian stage). Zoolog. Sci. 21, 285–298.

Delsuc, F., Brinkmann, H., Chourrout, D., Philippe, H., 2006. Tunicates and not cephalochordates are the closest living relatives of vertebrates. Nature 439, 965–968.

Dong, B., Horie, T., Denker, E., Kusakabe, T., Tsuda, M., Smith, W.C., Jiang, D., 2009. Tube formation by complex cellular processes in *Ciona intestinalis* notochord. Dev. Biol. 330, 237–249.

Hirano, T., Nishida, H., 2000. Developmental fates of larval tissues after metamorphosis in the ascidian, *Halocynthia roretzi*. II. Origin of endodermal tissues of the juvenile. Dev. Genes Evol. 210, 55–63.

Hotta, K., Mitsuhara, K., Takahashi, H., Inaba, K., Oka, K., Gojobori, T., Ikeo, K., 2007. A web-based interactive developmental table for the ascidian *Ciona intestinalis*, including 3D real-image embryo reconstructions: I. From fertilized egg to hatching larva. Dev. Dyn. 236, 1790–1805.

Irvine, S.Q., Cangiano, M.C., Millette, B.J., Gutter, E.S., 2007. Non-overlapping expression patterns of the clustered Dll-A/B genes in the ascidian *Ciona intestinalis*. J. Exp. Zool. B Mol. Dev. Evol. 308, 428–441.

Jefferies, R.P.S., 1986. The Ancestry of Vertebrates. British Museum, London.

Jeffery, W.R., 2006. Ascidian neural crest-like cells: phylogenetic distribution, relationship to larval complexity, and pigment cell fate. J. Exp. Zool. B Mol. Dev. Evol. 306, 470–480.

Jeffery, W.R., Chiba, T., Krajka, F.R., Deyts, C., Satoh, N., Joly, J.S., 2008. Trunk lateral cells are neural crest-like cells in the ascidian *Ciona intestinalis*: insights into the ancestry and evolution of the neural crest. Dev. Biol. 324, 152–160.

Katz, M.J., 1983. Comparitive anatomy of the tunicate tadpole, *Ciona intestinalis*. Biol. Bull. 164, 1–27.

Kourakis, M.J., Smith, W.C., 2007. A conserved role for FGF signaling in chordate otic/atrial placode formation. Dev. Biol. 312, 245–257.

Lancaster, E.R., Willey, A., 1890. The development of the atrial chamber of amphioxus. Q. J. Micro. Sci. 31, 445–466.

Locascio, A., Aniello, F., Amoroso, A., Manzanares, M., Krumlauf, R., Branno, M., 1999. Patterning the ascidian nervous system: structure, expression and transgenic analysis of the CiHox3 gene. Development 126, 4737–4748.

Manni, L., Lane, N.J., Zaniolo, G., Burighel, P., 2002. Cell reorganisation during epithelial fusion and perforation: the case of ascidian branchial fissures. Dev. Dyn. 224, 303–313.

Manni, L., Lane, N.J., Joly, J.S., Gasparini, F., Tiozzo, S., Caicci, F., Zaniolo, G., Burighel, P., 2004. Neurogenic and non-neurogenic placodes in ascidians. J. Exp. Zool. B Mol. Dev. Evol. 302, 483–504.

Manni, L., Mackie, G.O., Caicci, F., Zaniolo, G., Burighel, P., 2006. Coronal organ of ascidians and the evolutionary significance of secondary sensory cells in chordates. J. Comp. Neurol. 495, 363–373.

Mansour, S.L., Schoenwolf, G.C., 2005. Morphogenesis of the inner ear. In: Kelley, M.W., Wu, D.K., Popper, A.N., Fay, R.R. (Eds.), Development of the Inner Ear. Springer-Verlag, New York, pp. 43–84.

Mazet, F., Shimeld, S.M., 2005. Molecular evidence from ascidians for the evolutionary origin of vertebrate cranial sensory placodes. J. Exp. Zool. B Mol. Dev. Evol. 304, 340–346.

Mazet, F., Hutt, J.A., Milloz, J., Millard, J., Graham, A., Shimeld, S.M., 2005. Molecular evidence from *Ciona intestinalis* for the evolutionary origin of vertebrate sensory placodes. Dev. Biol. 282, 494–508.

Meinertzhagen, I.A., Okamura, Y., 2001. The larval ascidian nervous system: the chordate brain from its small beginnings. Trends Neurosci. 24, 401–410.

Meyers, E.N., Martin, G.R., 1999. Differences in left–right axis pathways in mouse and chick: functions of FGF8 and SHH. Science 285, 403–406.

Morokuma, J., Ueno, M., Kawanishi, H., Saiga, H., Nishida, H., 2002. HrNodal, the ascidian nodal-related gene, is expressed in the left side of the epidermis, and lies upstream of HrPitx. Dev. Genes Evol. 212, 439–446.

Northcutt, R.G., Gans, C., 1983. The genesis of neural crest and epidermal placodes: a reinterpretation of vertebrate origins. Q. Rev. Biol. 58, 1–28.

Okada, T., Yamamoto, M., 1999. Differentiation of the gonad rudiment into ovary and testis in the solitary ascidian, *Ciona intestinalis*. Dev. Growth Differ. 41, 759–768.

Ostrovsky, D., Sanger, J.W., Lash, J.W., 1983. Light microscope observations on actin distribution during morphogenetic movements in the chick embryo. J. Embryol. Exp. Morphol. 78, 23–32.

Putnam, N.H., Butts, T., Ferrier, D.E., Furlong, R.F., Hellsten, U., Kawashima, T., Robinson-Rechavi, M., Shoguchi, E., Terry, A., Yu, J.K., Benito-Gutierrez, E.L., Dubchak, I., Garcia-Fernandez, J., Gibson-Brown, J.J., Grigoriev, I.V., Horton, A.C., de Jong, P.J., Jurka, J., Kapitonov, V.V., Kohara, Y., Kuroki, Y., Lindquist, E., Lucas, S., Osoegawa, K., Pennacchio, L.A., Salamov, A.A., Satou, Y., Sauka-Spengler, T., Schmutz, J., Shin, I.T., Toyoda, A., Bronner-Fraser, M., Fujiyama, A., Holland, L.Z., Holland, P.W., Satoh, N., Rokhsar, D.S., 2008. The amphioxus genome and the evolution of the chordate karyotype. Nature 453, 1064–1071.

Schlosser, G., 2002. Development and evolution of lateral line placodes in amphibians I. Development. Zoology (Jena) 105, 119–146.

Schlosser, G., 2005. Evolutionary origins of vertebrate placodes: insights from developmental studies and from comparisons with other deuterostomes. J. Exp. Zool. B Mol. Dev. Evol. 304, 347–399.

Shimeld, S.M., Holland, P.W., 2000. Vertebrate innovations. Proc. Natl. Acad. Sci. U. S. A. 97, 4449–4452.

Shimeld, S.M., Levin, M., 2006. Evidence for the regulation of left–right asymmetry in *Ciona intestinalis* by ion flux. Dev. Dyn. 235, 1543–1553.

Streit, A., 2004. Early development of the cranial sensory nervous system: from a common field to individual placodes. Dev. Biol. 276, 1–15.

Streit, A., 2007. The preplacodal region: an ectodermal domain with multipotential progenitors that contribute to sense organs and cranial sensory ganglia. Int. J. Dev. Biol. 51, 447–461.

Turon, X., Lopez-Legentil, S., 2004. Ascidian molecular phylogeny inferred from mtDNA data with emphasis on the Aplousobranchiata. Mol. Phylogenet. Evol. 33, 309–320.

Wada, H., Satoh, N., 1994. Details of the evolutionary history from invertebrates to vertebrates, as deduced from the sequences of 18S rDNA. Proc. Natl. Acad. Sci. U. S. A. 91, 1801–1804.

Wada, H., Saiga, H., Satoh, N., Holland, P.W., 1998. Tripartite organization of the ancestral chordate brain and the antiquity of placodes: insights from ascidian Pax-2/5/8, Hox and Otx genes. Development 125, 1113–1122.

Willey, A., 1893. Studies on the Protochordata. I. On the origin of the branchial stigmata, preoral lobe, endostyle, atrial cavities, etc., in *Ciona intestinalis*, Linn, with remarks on *Clavelina lepadoformis*. Q. J. Micro. Sci. 43, 317–360.